Journal of Building Engineering 82 (2024) 108168

Contents lists available at ScienceDirect

Journal of Building Engineering

journal homepage: www.elsevier.com/locate/jobe

Simulation of a radiation-enhanced thermal diode tank (RTDT) assisted refrigeration and air-conditioning (RAC) system using TRNSYS

Mingzhen Wang, Eric Hu *, Lei Chen

School of Electrical and Mechanical Engineering, the University of Adelaide, SA 5005, Adelaide, Australia

ARTICLE INFO

Keywords:
Cooling system
Thermal diode tank
TRNSYS simulation
Cold energy storage
WSHP

ABSTRACT

The increasing demands for refrigeration and cooling have led to higher energy consumption and greenhouse gas emissions of Refrigeration and Air-conditioning (RAC) systems. To tackle this global challenge, a Radiation-enhanced Thermal Diode Tank (RTDT) has been proposed as an innovative and sustainable condenser-cooling approach to assist the RAC system to save energy. The RTDT is a passive cooling device that utilises a Radiation-enhanced Heat Pipe (RHP) to discharge heat in one direction, i.e., from the interior of a heat-insulated water tank to the surrounding area. In this paper, TRNSYS simulation was used to conduct a case study comparing the performance of the RTDT assisted RAC (RTDT-RAC) system with a reference Air-cooled RAC system under identical ambient conditions in Adelaide, Australia. The findings show that the RTDT-RAC system can save up to 40 % energy compared with the reference RAC system, with an increased Coefficient of Performance (COP) of 5.34. Moreover, a parametric analysis has also been conducted to study the impacts of weather conditions or regions, room temperature setpoints and RHP radiative surface areas on the RTDT-RAC system's performance. The results of the parametric analysis indicate that the regions with larger day and night ambient temperature differences demonstrate better energy-savings. Both a higher room temperature setpoint and an increased RHP radiative surface area can increase the energy-savings effectively. For a 50 m^3 RTDT, to achieve energy-savings, the RHP radiative surface area is found to be at least 2.2 m^2, while the optimal value is about 5 m^2.

1. Introduction

Over the past decades, cold energy storage has become a fundamental solution for thermal energy management for energy conservation [1]. Among the innovative approaches in this field, the Thermal Diode Tank (TDT) has been proposed as a cold energy storage system specifically designed to supply cooling water and reduce the condensing temperature in Refrigeration and Air-conditioning (RAC) systems. With a heat pipe implemented, the heat is dissipated from the TDT water to the external surroundings unidirectionally, which serves as a thermal diode. The reason for reducing the condensing temperature is because extensive research has demonstrated that condenser-cooling technology is a validated and effective method for improving the Coefficient of Performance (COP) of RAC systems [2]. Such condenser-cooling approaches include evaporative cooling [3–11], ground-sourced cooling [12–17] and water-sourced cooling [18–20]. The TDT was specifically designed as an innovative alternative to conventional water-sourced

* Corresponding author.
E-mail address: eric.hu@adelaide.edu.au (E. Hu).

https://doi.org/10.1016/j.jobe.2023.108168
Received 29 August 2023; Received in revised form 31 October 2023; Accepted 14 November 2023
Available online 18 November 2023

cooling techniques. It was verified that a TDT assisted RAC (TDT-RAC) system could save up to 40 % energy compared with a reference RAC system [21]. The key component of a TDT is the heat pipe, which transfers heat unidirectionally from the tank water to the surroundings. Furthermore, enhancing the heat transfer capability of the heat pipe can lead to significant improvements in the TDT-RAC system performance. Building upon this knowledge, a Radiation-enhanced Heat Pipe (RHP) has been recently introduced to replace the standard heat pipe in a TDT-RAC system. The RHP is specifically designed to enhance heat transfer through radiation from the night sky. Therefore, the Radiation-enhanced Thermal Diode Tank (RTDT), incorporating the RHP, represents a substantial advancement in cold energy storage, and the RTDT is able to achieve even lower water temperatures [22,40].

In this study, a comprehensive powerful simulation software for dynamic modelling called Transient System Simulation Program (TRNSYS) has been used to simulate the TDT-RAC system. It is widely applied to solve multi-component compound systems, such as solar (solar thermal and photovoltaic systems) systems, Ground-sourced heat pump (GSHP) air conditioning systems, thermal/cold energy storage systems and Combined Cooling and Heating Power (CCHP) systems. A solar driven ejector cooling system with Phase Change Materials (PCM) was simulated through TRNSYS modelling by Allouche et al. [23]. They found the highest COP and solar thermal ratios were 0.193 and 0.097, and the optimal PCM storage volume was found to be 1000 L. A TRNSYS simulation of a solar-assisted air-conditioning system integrated with a thermal energy storage tank (Type 71 for a solar collector and Type 534 for a storage tank) was developed by Aguilar-Jiménez et al. [24], which predicted that the system could operate continuously with no more than 75 % of the cooling capacity, with the cooling tower requiring 750 kg of water every day. A residential house in Tunisia coupled with a heat pump system (Type 56a) was investigated by Chargui and Sammouda [25] using a TRNSYS model, with a water storage tank involved. The results showed that under the given situation, the COP of the heat pump was from 6 to 9, and the outlet water temperature was 55 °C. Moreover, they found the heat pump COP, system COP, room temperature and energy inside the house all increased if the tank water temperature increased. Chargui et al. [26] also presented a TRNSYS model to simulate the temporal evolution of delivered power, consumed power and COP of the heat pump system. Their simulation revealed that the above-mentioned three parameters reached the maxima between the 10th and 15th hour within 24 h, and the maximum COP was found to be around 4. A reversible water-to-water heat pump was modelled by Bordignon et al. [27] using TRNSYS (Type 534 for water tank). In their study, the seasonal COP of the heat pump system with different configurations (single-stage and cascade cycles) for a 10-year simulation were found, and the evaporation and condensation temperatures and pressures were presented for a 5-year simulation. Hou et al. [28] used TRNSYS (Type 919) to present a hybrid GSHP system model and found the system COP was stable at 3.3, which was deemed to be better than a conventional GSHP system. A TRNSYS simulation on PCM-enhanced walls (Type 285) was studied by Al-Saadi and Zhai [29], from which they found the maximum savings on annual cooling could be up to 15.8 %.

Brough et al. [30] used TRNSYS to simulate a heat pipe heat exchanger system (Type 202), and the simulated results of the inlet and outlet fluid temperature of the installed system were compared with their experimental data. They found that the simulation results were within an average of 4.4 % error. Ahamed et al. [31] developed a TRNSYS model to predict the heating requirements for a conceptual greenhouse, and their simulation was compared with another validated heating simulation model, while the average error between the two models was approximately 5 %. A TRNSYS model on PCM walls (Type 260) was presented by Kuznik et al. [32] and validated by experimental data with good agreement. However, they summarised that the model could not predict the phase change in the microcapsule. Fang et al. [33] compared TRNSYS simulation data and monitoring data of the energy consumption, indoor temperature and relative humidity of a construction combined with floor radiant cooling. The results revealed that the simulation data matched with the monitoring data with good agreement, verifying that this TRNSYS simulation was credible. A solar assisted heat pump system coupled with a water tank was simulated by Banister et al. [34] based on TRNSYS and also validated with experimental data. Their comparison revealed that the typical error in average water tank temperature was below 1 °C. A TRNSYS model on an HVAC control system was simulated by Lin et al. [35] who suggested that this model could reduce annual electricity consumption by up to 40 % and reduce boiler energy consumption by around 35 %. A TRNSYS simulation of a solar domestic hot water system (Type 60 d) was developed by Haurant et al. [36] and also validated from the monitoring data. The results of inlet and outlet water temperatures and power showed that the simulation was in general agreement with the experimental data across 18 h. A water storage tank coupled with PCM was simulated in TRNSYS by Bony and Citherlet [37], where the simulation results matched well with their experimental data, from the perspective of the measured temperature in the PCM module. Another validation of the TRNSYS simulation of a hot water storage tank (Type 860) with PCM was conducted by Nkwetta et al. [38], which also announced good agreement. In the TRNSYS simulation platform, the modularity of the system is a fundamental feature, with each individual component represented by a unique “type number”. These type numbers serve as distinct identifiers for various components within the system, allowing for precise modelling and analysis. In previous works mentioned above, the core components have been identified, each associated with its respective type number. These core components encompass critical elements of the simulated system, such as heat exchangers, heat pumps, and more. This emphasis has provided valuable insights and a foundation for the research presented in this study.

The research and application of TRNSYS in HVAC systems is ongoing and varied. The literature mentioned above demonstrates that TRNSYS has been extensively used to simulate energy-efficiency incorporating different heat pump systems, solar-driven systems and different thermal storage tanks. However, although the RTDT assisted RAC (RTDT-RAC) system was previously proposed in existing works, it has not been simulated under dynamic conditions, neither in TRNSYS nor other dynamic simulation tools. Therefore, this paper aims to demonstrate the ascendancy of the proposed RTDT-RAC system over a reference RAC system by developing two TRNSYS performance simulation models. A case study based on summer weather data in Adelaide, Australia, was carried out to compare the difference in energy efficiency between the simulation models. Additionally, to obtain a better understanding of how the design and operational parameters impact the performance of the integrated system, a parametric analysis was conducted. The study is expected to provide insights into the overall energy efficiency of the RTDT-RAC system and identify the potential optimal design and operational conditions that can yield significant energy-savings.

2. RTDT-RAC system description

The Radiation-enhanced Thermal Diode Tank (RTDT) is designed to passively reject heat energy to the external environment at night and store cold water, which can later be used for lowering the condensing temperature of the RAC system. The proposed RTDT consists of an adiabatic water tank and a Radiation-enhanced Heat Pipe (RHP), as depicted in Fig. 1. The RHP typically use R134a as its working fluid that undergoes phase changes during operation, and its working temperature ranges from roughly −20 °C–100 °C under standard atmospheric pressure. The evaporator of the RHP is a hollow cylindrical tube, and the condenser is a hollow cuboid with a large flattened surface facing to the sky. When the water temperature is above the ambient air and sky temperatures, the RHP will start transferring heat from the water to its surroundings. Conversely, the RHP ceases its operation when the ambient temperature rises above the water temperature. As the tank walls are ideally well-insulated, heat does not enter the tank interior through the walls. In addition, the RHP offers a large flattened hollow cuboid as its condenser section to radiate heat to the night sky, while maintaining convection heat transfer with the air. Notably, the temperature of the night sky is typically lower than the ambient temperature at ground level. Therefore, when the RTDT-RAC system is deployed outdoors overnight, the radiative cooling effect allows the RTDT water temperature to decrease below the ambient temperature. This additional cooling mechanism further enhances the system's overall energy efficiency and performance [21,22].

A reference conventional Air-cooled RAC system, System 1, shown in Fig. 1 (left part), incorporates a standard condenser and evaporator components with a compressor to facilitate the heat dissipation, heat absorption and power input, respectively. As the condenser is the main component to dissipate heat, a conventional RAC system normally utilises a fan to enhance the air flow rate, and hence improve the heat dissipation at the condenser part. The evaporator, on the other hand, absorbs heat from the conditioned space, allowing for cooling within the area.

When the RTDT is applied in a reference RAC system, the tank water is supplied to the condenser of the RAC system through pipes, and the outdoor fan is removed. Hence, the cooling water lowers the condensing temperature directly, instead of cooling the condenser using ambient air. Such integration constitutes an RTDT-RAC system (System 2 shown in the whole part of Fig. 1) incorporating a water-cooled condenser that receives the cooling water from the RTDT. It is noted that the evaporator of System 2 is the same as that of System 1. During the night, after the water is heated and pumped back to the RTDT, the water temperature is higher than both the ambient air and the sky temperatures. Therefore, the RHP then transfers heat from the RTDT water to the external environment. Following this working principle, the RTDT water is theoretically cooled to a temperature that is even lower than the minimum ambient temperature at night. Eventually, it becomes ready for system operation the following day.

3. Study case

The study case comprises an office in Adelaide, Australia, with a room area of 500 m^2, which was maintained at a constant room temperature for 8 h per day from 9 a.m. to 5 p.m., during the Australian summer months (January to March). The office was conditioned by System 1 (a reference Air-cooled RAC system), and the proposed System 2 (the RTDT-RAC system with a 50 m^3 RTDT), respectively. To demonstrate the benefits of the energy efficiency of System 2 when compared with System 1, TRNSYS was used for system simulations. The detailed specifications of the building are given in Table 1, where the room temperature setpoint is 22 °C. The required cooling capacity to condition the room would vary time-dependently based on the ambient conditions. Based on both the ambient conditions and the room temperature setting, both System 1 and System 2 are rated with a cooling capacity of 28.5 kW. With this rated cooling capacity of 28.5 kW, both systems are expected to be capable of providing sufficient cooling power to meet the specified requirements and maintain the desired room temperature. Further information about the RAC system and RTDT is given in Table 2 and Table 3. The simulation model for System 2 in the study case also contains the impact of the RTDT volume, which is set at

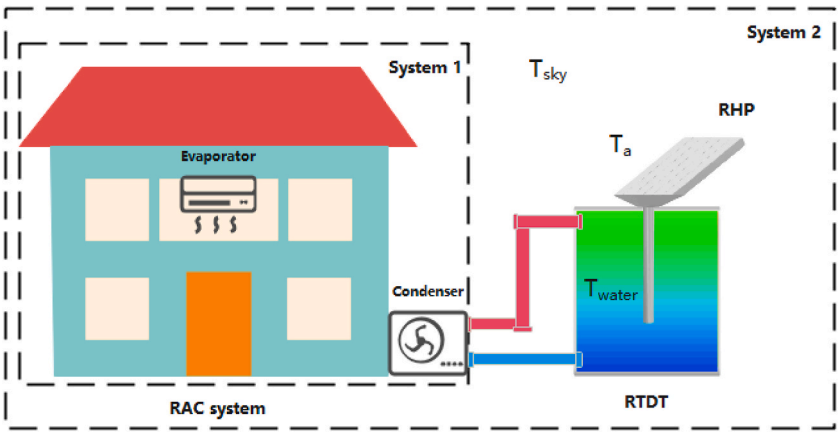

Fig. 1. Schematics of a reference Air-cooled RAC system (System 1), and the proposed RTDT-RAC system (System 2). During the day, when System 2 is running, the condenser is cooled by the cooling water from RTDT and the water is gradually heated. Once T_{water} is higher than T_a or T_{sky}, heat dissipates from the RTDT water to ambient air and sky through the RHP. Otherwise, the RHP is non-operational. This heat dissipation process occurs effectively, especially during the night when T_a is lower than T_{water}. On subsequent days, when the RAC system begins operating, the cooled RTDT water is then used to cool the RAC system's condenser.

Table 1
Building information for the case study.

Building information	
Window-to-Wall ratio	East: 0.3 West: 0.3 South: 0.34 North: 0.34
Conditioned room	Area: 500 m^2
Thermal parameters of envelope	External wall heat transfer coefficient: 0.65 W/m^2K External window heat transfer coefficient: 2.5 W/m^2K Roof heat transfer coefficient: 0.32 W/m^2K Floor-to-ground thermal resistance: 0.625 $(m^2K)/W$ External window solar heat gain coefficient: 0.25
Internal thermal gain	People: 6 W/m^2 Device (computers, tv … etc.): 10 W/m^2 Lighting: 8 W/m^2
System set point	Heating: 22 °C Cooling: 22 °C Monitoring temperature: 22 °C
Relative humidity	60 %

50 m^3, as well as the RHP radiative surface area for dissipating heat from the water tank to the surroundings, which is set at 15 m^2. The RHP radiative surface is characterized by a grey body with an emittance of 0.7, and an absorptance of 0.7. Taking into account these parameters, TRNSYS offered a comprehensive performance analysis of the two systems, including their COP values, cooling power, system power and overall energy-savings.

To evaluate the performance of Systems 1 and 2 based on the TRNSYS simulations, some key performance indicators have been determined, including the system COP, cooling power and the energy consumption. The following equations have demonstrated the derivation of the system COP.

$$\dot{W}_{system1} = \dot{W}_{c1} + \dot{W}_{fan\_in} + \dot{W}_{fan\_out} \tag{1}$$

$$COP_{air} = \frac{\dot{Q}_{cooling1}}{\dot{W}_{system1}} \tag{2}$$

where $\dot{W}_{system1}$ represents the total input power of System 1, $\dot{W}_{c1}$ is its compressor power, $\dot{W}_{fan\_in}$ and $\dot{W}_{fan\_out}$ are the indoor and outdoor fan power, and $\dot{Q}_{cooling1}$ is the cooling power to the room provided by System 1. All these parameters have the same unit of kJ/hr or kW.

$$\dot{W}_{system2} = \dot{W}_{c2} + \dot{W}_{blower} + \dot{W}_{waterpump} \tag{3}$$

$$COP_{water} = \frac{\dot{Q}_{cooling2}}{\dot{W}_{system2}} \tag{4}$$

where $\dot{W}_{system2}$ is the total input power of System 2, $\dot{W}_{c2}$ is its compressor power, $\dot{W}_{blower}$ is the blower power and $\dot{W}_{waterpump}$ is the power of the water pump. All these parameters have the same unit of kJ/hr or kW.

The saved power and the Energy Saving Percentage (ESP) can be expressed as follows:

Table 2
RAC systems information.

Name	Value	Unit
Air-cooled RAC system information		
Refrigerant	R410A	–
Rated total cooling capacity	28.5	kW
Total air flow rate	6110	m^3/hr
Rated indoor fan power	0.689	kW
Rated outdoor fan power	0.689	kW
RTDT-RAC system information		
Refrigerant	R410A	–
Rated total cooling capacity	28.5	kW
Total air flow rate	4800	m^3/hr
Total liquid flow rate	6.48	m^3/hr
Density of liquid stream (water)	1000	kg/m^3
Specific heat of liquid stream (water)	4.19	kJ/kgK
Rated blower (indoor fan) power	0.3	kW

Table 3
RTDT information for the case study.

RTDT information		
Name	Value	Unit
RTDT volume	50	m^3
RTDT height	3	m
RTDT loss coefficient (top, edge and bottom)	0.4	W/m^2K
RHP total area	15	m^2
RHP fin efficiency factor	0.7	–
RHP loss coefficient (top, edge and bottom)	3.0	kJ/hr. m^2K
Radiative surface emittance	0.7	–
Radiative surface absorptance	0.7	–
Fluid (water) specific heat	4.19	kJ/kgK
Fluid (water) density	1000	kg/m^3
Fluid (water) thermal conductivity	2.224	kJ/hr.mK
Fluid (water) flow rate	6.48	m^3/hr
Water pump power	0.38	kW

$$\dot{W}_{saved} = \dot{W}_{system1} - \dot{W}_{system2} \tag{5}$$

$$ESP = \frac{\dot{W}_{system1} \times t_a - \dot{W}_{system2} \times t_w}{\dot{W}_{system1} \times t_a} \times 100\% \tag{6}$$

where t_a and t_w represent the total operation period of Systems 1 and 2.

4. TRNSYS simulation

TRNSYS (TRaNsient SYstem Simulation) was developed by the Solar Energy Laboratory at the University of Wisconsin-Madison [39]. With a library of pre-built components representing system elements, TRNSYS enables the creation of customised models and simulates both steady-state and dynamic behaviour.

In this study, two systems were simulated by TRNSYS 18 under dynamic conditions and all input and output data are hourly based. The Type 15–2 component provided weather data such as the ambient (dry bulb) temperature, effective sky temperature, humidity, and solar radiation to the models. The Building component (Type 56) represented the office room being conditioned and included input parameters such as the thermal parameters of building envelopes, initial room temperature and internal loads. The online plotter

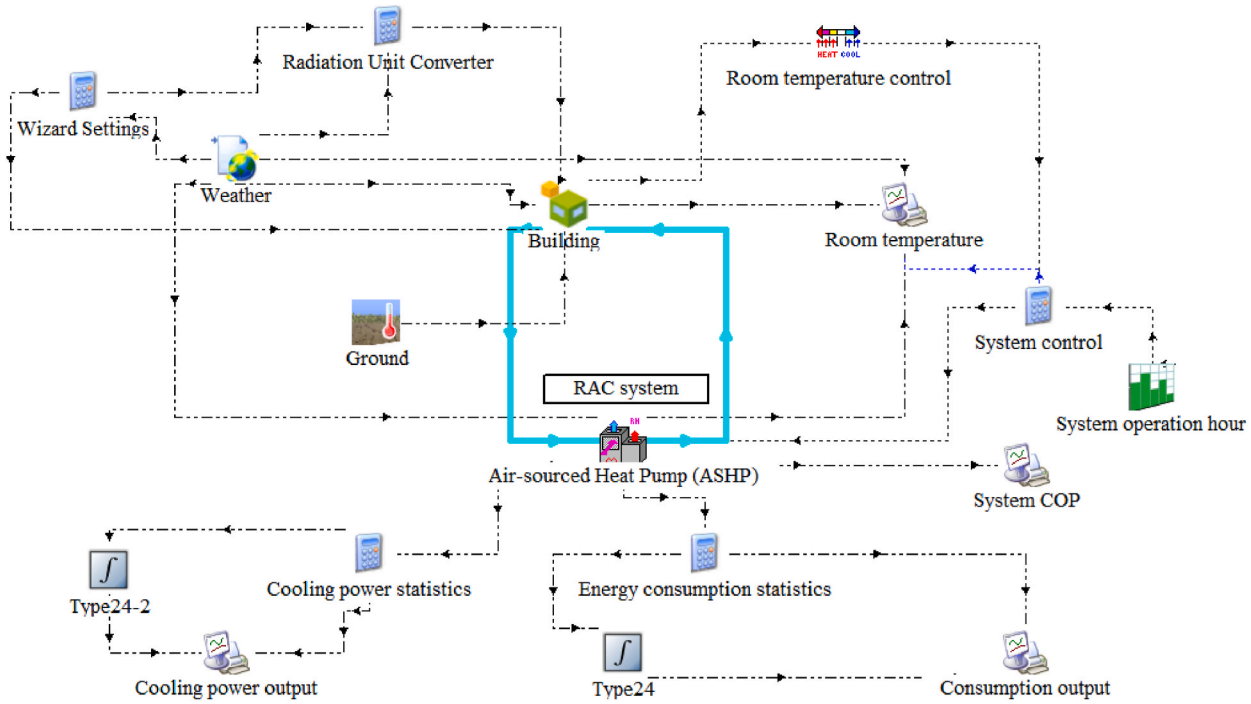

Fig. 2. Reference Air-sourced RAC system (System 1) by TRNSYS simulation.

enabled visualisation of the results in real-time. The Type 77 component provided the ground/soil temperature for the building.

For the TRNSYS model for System 1, shown in Fig. 2, the Type 954c component is selected as the module of a reference air-cooled RAC system to provide cooling to the office room, which is an Air-sourced Heat Pump (ASHP). The ASHP component uses R410A as its refrigerant and its rated total cooling capacity is set as 28.5 kW. Other inputs of the ASHP component align with the specifications given in Table 2. It also takes in the time-dependent ambient conditions from the Weather component, cooling capacity from the Building component, and ground temperature from the Ground component. Then, the ASHP component outputs the temperature data, COP, cooling power and energy consumption from System 1.

For the TRNSYS model of System 2, shown in Fig. 3, a Type 919 component is selected to provide cooling as a Water-sourced Heat Pump (WSHP), which is connected to a thermal storage tank (e.g., TDT) via a water pump to control the water loop. Input parameters for this WSHP include the ambient conditions from the Weather component, water loop (in and out) temperatures from the Thermal Storage Tank component, cooling capacity from the Building component, water flow rate from the Water Pump component and ground temperature from the Ground component. The refrigerant and rated total cooling capacity of the WSHP component are the same as those of the ASHP component for System 1. The RTDT is integrated via a thermal storage tank (Type 158 component as a TDT) filled with water, and a solar thermal collector (Type 1 component as an RHP). The thermal collector component takes in the effective sky temperature from the Weather component as its ambient temperature, in order to radiate heat from the water to sky. Therefore, as long as the temperature of water in the thermal storage tank is higher than the effective sky temperature, the heat in the water would be dissipated to the external environment. An additional condition has been added to the RTDT unit by an ON/OFF Differential Controller, Type 165 component. The condition is that when either the ambient or effective sky temperature is higher than the water temperature, the emittance and absorptance of the thermal collector both become zero. This indicates the null operation of the thermal collector, so that no more heat from the ambient air will enter the thermal storage tank through the thermal collector. However, whenever the ambient and effective sky temperatures become lower than the water temperature, the emittance and absorptance of the thermal collector are set to default (both to 0.7). The details of the RTDT unit in this TRNSYS model align with the specifications outlined in Table 3. By offering this condition, the integration of the thermal storage tank and the solar thermal collector can function as the proposed RTDT. The outputs that the WSHP component can provide include temperature data, COP, cooling power and energy consumption. More details about the applied TRNSYS components are outlined in Table 4.

5. Results and discussion

Using TRNSYS modelling, the hourly results of Systems 1 and 2 have been obtained over the summer season (Jan–Mar) in Adelaide, Australia, including the (ambient, room, supply air and RTDT water) temperature data, system COP, cooling power and energy consumption.

5.1. Temperature data

The TRNSYS simulations have plotted the temperature histories of Systems 1 and 2 over three summer months, as shown in Fig. 4. From Fig. 4a, it can be observed that for System 1 (the reference Air-cooled RAC system), the room temperature during the daytime of

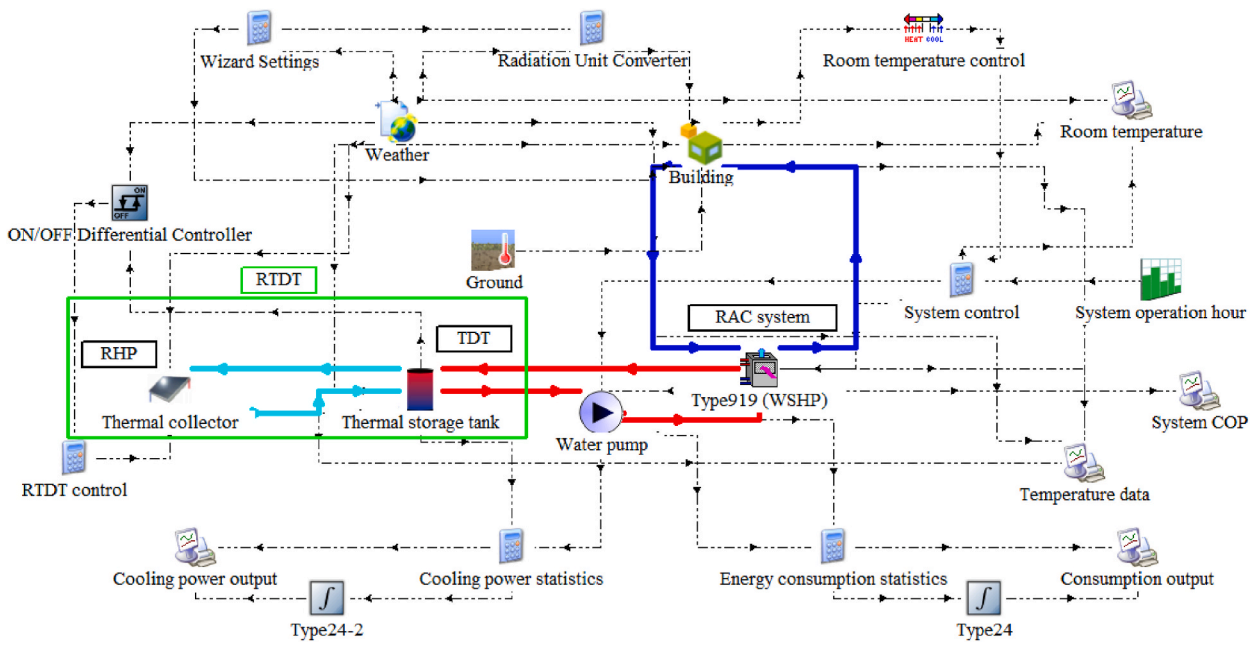

Fig. 3. Proposed RTDT-RAC system (System 2) by TRNSYS simulation.

Table 4
Standard TRNSYS components.

Component Name	TRNSYS Type	Comments
Weather	Type 15-2	Adelaide weather data from 2023.01.01 to 2023.03.01, including ambient (dry/wet bulb) temperature, effective sky temperature, humidity, and solar radiation.
Building	Type 56	A multi-Zone building that aligns with the specifications in Table 1.
Online plotter	Type 65c	Online graphical plotter with output file.
System operation hour	Type 14	Time-dependent forcing function to control the RAC system operation duration from 9 a.m. to 5 p.m. each day.
Room temperature control	Type 108	Room thermostat for fixing the room temperature setpoint at 22 °C
Ground	Type 77	Soil temperature profile
ASHP	Type 954	Air sourced heat pump model with normalized capacity, which aligns with the ASHP specifications in Table 2.
WSHP	Type 919	Water sourced heat pump model with normalized capacity, which aligns with the WSHP specifications in Table 2.
Water pump	Type 114	Single speed pump for water circulation at a rated water flow rate of 6480 kg/h.
Thermal storage tank	Type 158	Cylindrical storage tank that aligns with the specifications in Table 3.
Thermal collector	Type 1	Solar collector with quadratic efficiency and the 2nd order incidence angle modifiers, which aligns with the specifications in Table 3.
ON/OFF Differential Controller	Type 165	If ambient or effective sky temperature $\geq$ water temperature, thermal collector is off. Otherwise, thermal collector is on.

each day is controlled below the ambient temperature within the range of 20 °C–22 °C when the highest ambient temperature is below 35 °C. This indicates that the required cooling capacity has been satisfied and the room is successfully conditioned as intended. However, when the ambient temperature exceeds 35 °C, the room temperature does not reach the desired level and ranges from 22 °C to 28 °C. This shows that the rated total cooling capacity of System 1 falls short in achieving the desired room temperature of around 22 °C. These observations highlight the limitations of System 1 in effectively managing higher ambient temperatures.

System 2 (RTDT-RAC system) exhibits comparable trends and faces similar challenges to System 1 when the ambient temperature surpasses 35 °C. However, notable differences are explored in the results. During system operation, the room temperature of System 2 is, on average, approximately 0.4 °C lower than that of System 1. Furthermore, the highest recorded room temperature in System 2 is around 1 °C lower than that in System 1. These findings indicate that System 2 achieves a slightly better temperature control performance with a marginally lower average room temperature and mitigation of temperature peaks.

5.2. System COP

The results of hourly COP values of Systems 1 and 2 are revealed in Fig. 5. For System 1, it is found that the COP values are within the range 1.9–3.3 during system operation. This range aligns with the typical COP values of commonly-used RAC systems, which generally fall between 1.5 and 4. Thus, the results obtained from this model are deemed acceptable. In contrast, System 2 exhibits a significantly higher COP, ranging from 4.1 to 6.3. On average, the monthly COP over the summer period of System 1 and System 2 are 2.52 and 5.34, respectively. This substantial improvement in COP for System 2 indicates an enhanced energy efficiency, compared with System 1.

5.3. Cooling power and energy consumption

The hourly cooling power and accumulated cooling energy of System 1 and System 2 over three summer months are presented in Fig. 6, where the cooling energy is calculated by multiplying the cooling power with the system operation period. For System 1, the average hourly cooling power is measured at 22.2 kW, and the system runs for a total of 449 h during the three-month period. The accumulated energy utilised for cooling purposes amounts to 9953 kWh.

In comparison, System 2 demonstrates a higher average hourly cooling power of 25.8 kW and operates for a slightly shorter duration of 439 h. The accumulated cooling energy for System 2 is determined to be 11,326 kWh. These results conclusively show that System 2 delivers greater cooling power than System 1, despite running for a slightly shorter period. This finding reinforces the earlier observation in Section 5.1, which proves that System 2 consistently maintains a lower conditioned room temperature, on average, than that achieved by System 1. The result confirms that System 2 has superior cooling performance by consistently providing more cooling and thereby achieving a lower conditioned room temperature.

Fig. 7 presents the power consumption within each hour and the accumulated energy consumption of System 1 and System 2 over a three-month period. The hourly power consumption of System 1 varies from 8.2 to 9.9 kW, with an average value of 8.8 kW during the system's operation. The accumulated energy consumption of System 1 amounts to 3961 kWh. On the other hand, System 2 exhibits hourly power consumption ranging from 4.6 to 6.7 kW, and its average hourly power consumption is found to be 5.4 kW. The accumulated energy consumption for System 1 and System 2 amounts to 3961 kWh and 2374 kWh, respectively. These results clearly indicate that while System 2 consumes less energy than System 1, it still provides a greater amount of cooling energy for conditioning the room. This finding unequivocally demonstrates the improved performance of System 2, as it delivers more cooling output while operating more efficiently.

The monthly results of energy consumption, system cooling energy and COP are listed in Table 5. In comparison with System 1, up to 1573 kWh of energy have been saved by System 2 over three months. The reduced energy consumption of System 2 also shows a mean Energy Saving Percentage (ESP) of 40 %, making it a promising and sustainable option for refrigeration and air-conditioning needs.

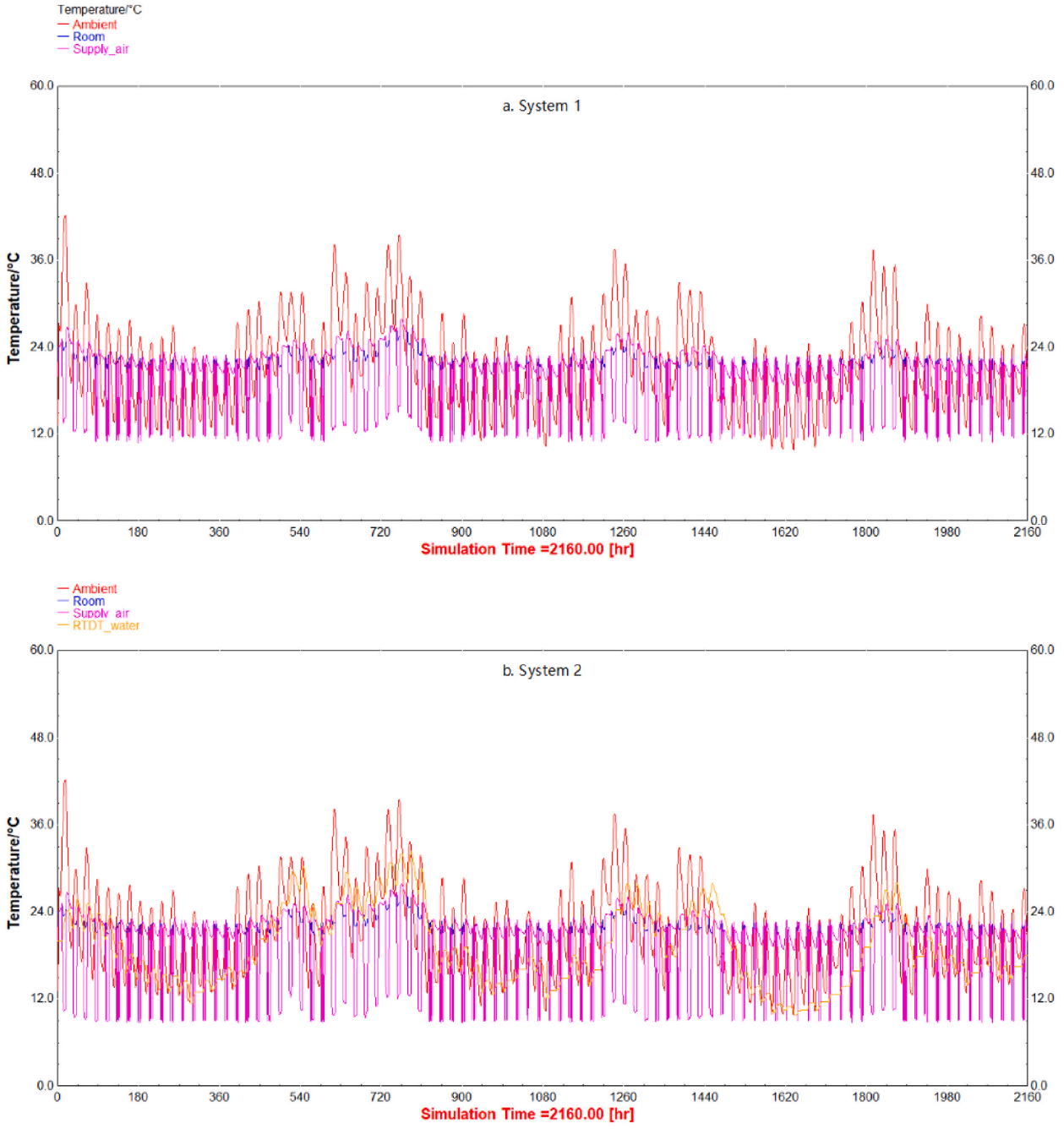

Fig. 4. Temperature histories of a) System 1, and b) System 2 over three months.

6. Parametric analysis

A parametric analysis has been conducted in order to investigate the impacts of region, room temperature setpoint, and RHP radiative surface area on the RTDT-RAC system (System 2) performance. Based on the results of the case study, Adelaide has been set as the Reference City for this parametric analysis. This systematic investigation also aims to identify the optimal configuration and operating conditions that can maximise the cooling efficiency of the RTDT-RAC system.

6.1. Region

Exploration of different locations enables understanding of how regional climate conditions affect the RTDT-RAC system's performance. Therefore, studies of some major cities in the southern hemisphere, such as Sydney, Rio de Janeiro, Brasilia, Cape Town and Santiago, have been conducted. The differences in ESP over three months (Jan–Mar) are shown in Fig. 8. Among these studied cities,

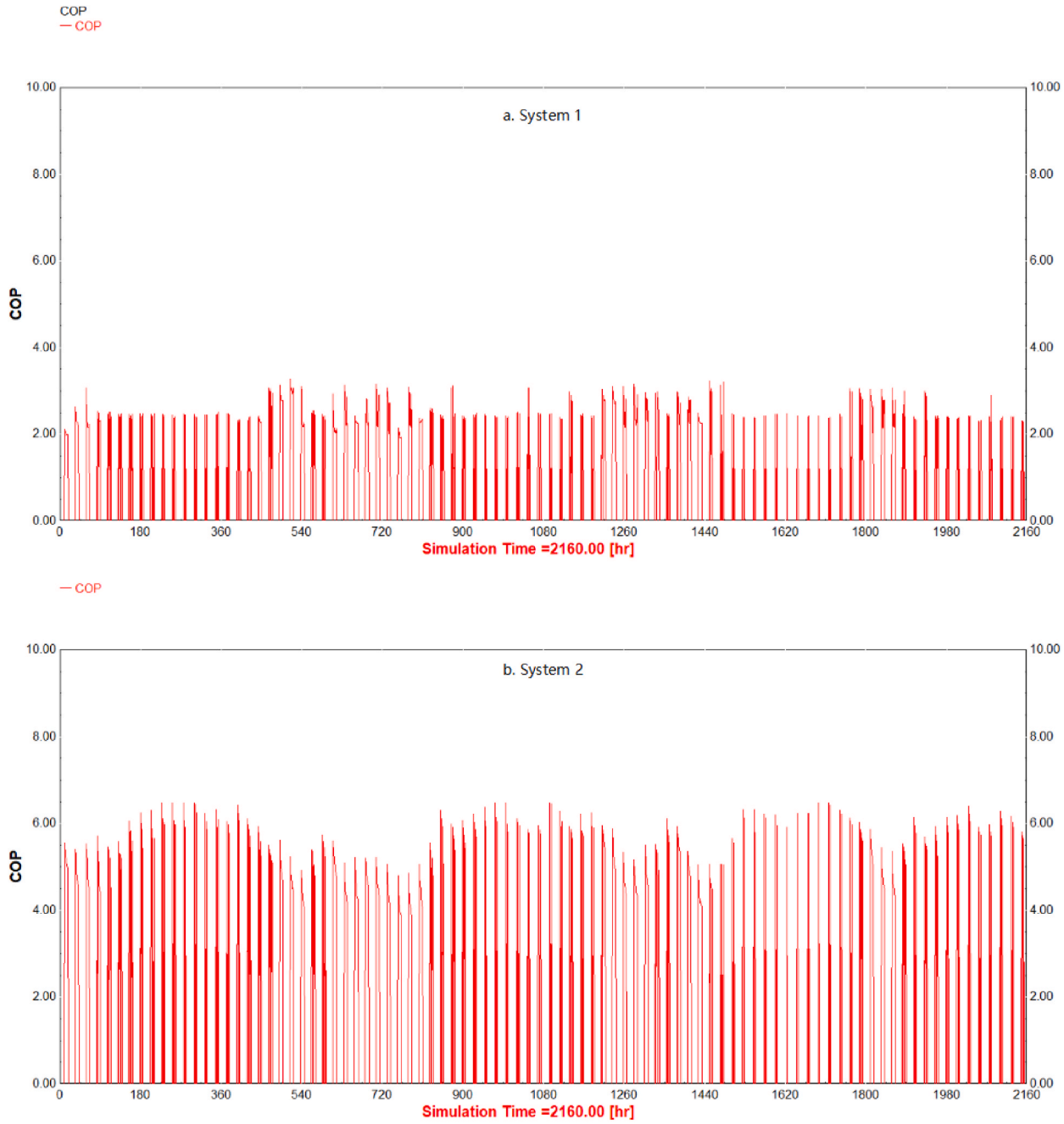

Fig. 5. Hourly COP of a) System 1, and b) System 2 over three months.

Santiago demonstrates the highest ESP, 44.0 %, followed by Cape Town and Adelaide, and they all achieve high ESPs above 40 %. These three cities share certain commonalities in their climate characteristics, in that they have a relatively larger day and night ambient temperature difference in the summer season. Moreover, coastal cities like Santiago, Cape Town and Adelaide may exhibit cooler nights due to their proximity to the ocean, alongside higher daytime temperatures.

Brasilia, Sydney, and Rio de Janeiro reveal decreasing ESP values, ranging from 28.9 % to 35.8 %. While these cities still benefit from energy-savings compared with the reference system, they show relatively lower energy efficiency than the top-performing cities. This is because the day and night temperature differences in these cities are less significant than in the top-performing cities.

The day and night ambient temperature difference is considered to be the major factor affecting the ESP of the RTDT-RAC system, as a lower night ambient temperature is more beneficial to reducing the RTDT water temperature. The lower the RTDT water temperature, the better the RTDT-RAC system performance will be. Moreover, factors such as cloud cover, precipitation patterns, and wind

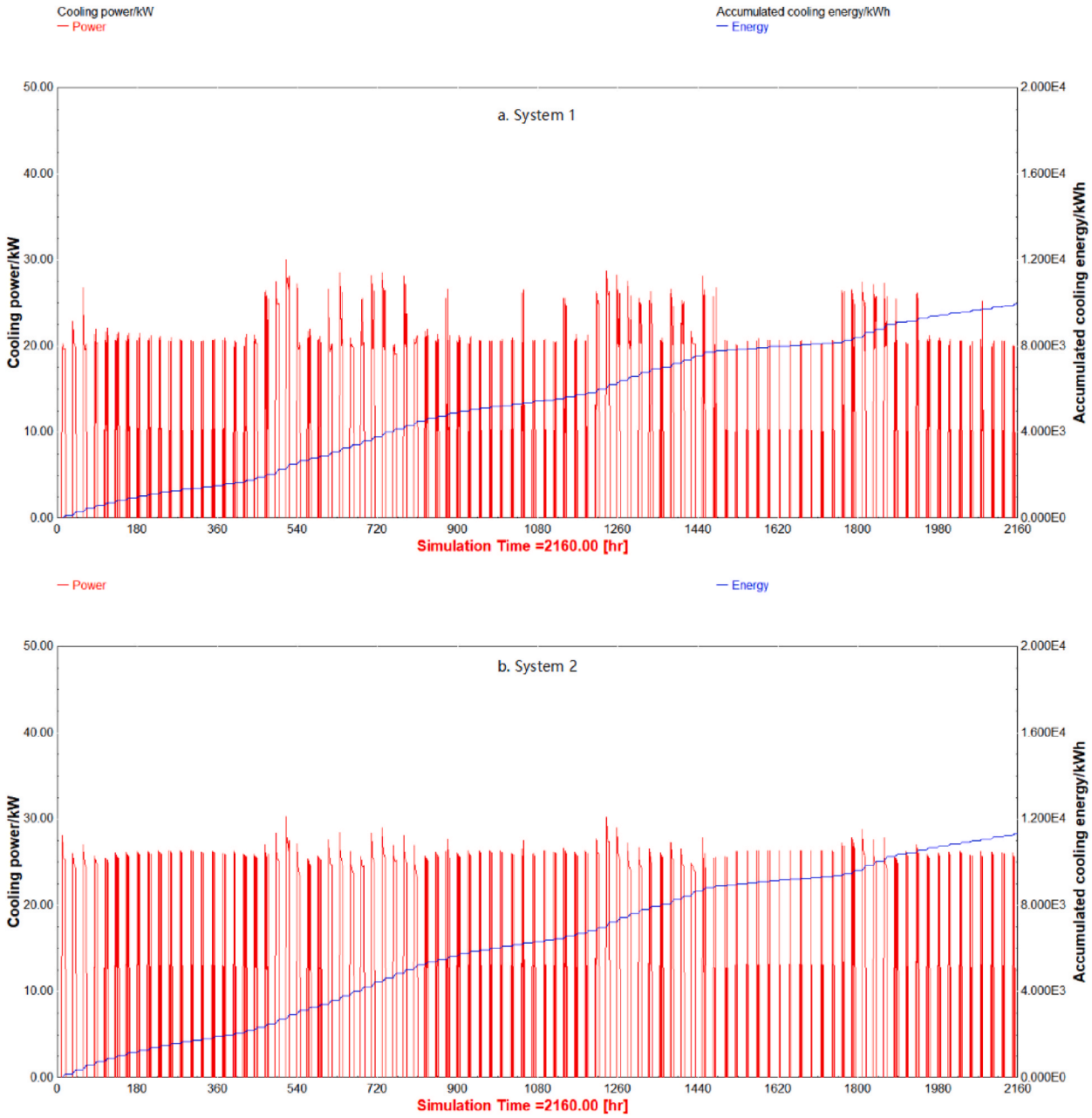

Fig. 6. Hourly cooling power and accumulated cooling energy of System 1 over 3 months.

can also influence the ESP of the RTDT-RAC system, but they are beyond the scope of this study.

6.2. *Room temperature setpoint*

The sensitivity of ESP on variable room temperature setpoints within a standard Air-conditioning Range from 18 °C to 26 °C in different regions is shown in Fig. 9. It is found that the ESP of the RTDT-RAC system increases as the room temperature setpoint increases for all studied regions. This finding suggests that higher room temperature setpoints are associated with greater energy-savings in the RTDT-RAC system. As the room temperature increases within a comfortable range, the cooling capacity for conditioning the space decreases. This reduction in cooling capacity results in lower energy consumption by both the reference and the RTDT-RAC systems. When evaluating the ESP, it is crucial to compare the energy consumption of the RTDT-RAC system with that of the reference Air-cooled RAC system. Although both systems may experience reductions in cooling capacity and energy consumption as the room temperature increases, the RTDT-RAC system has the potential to outperform the reference system in terms of energy-savings.

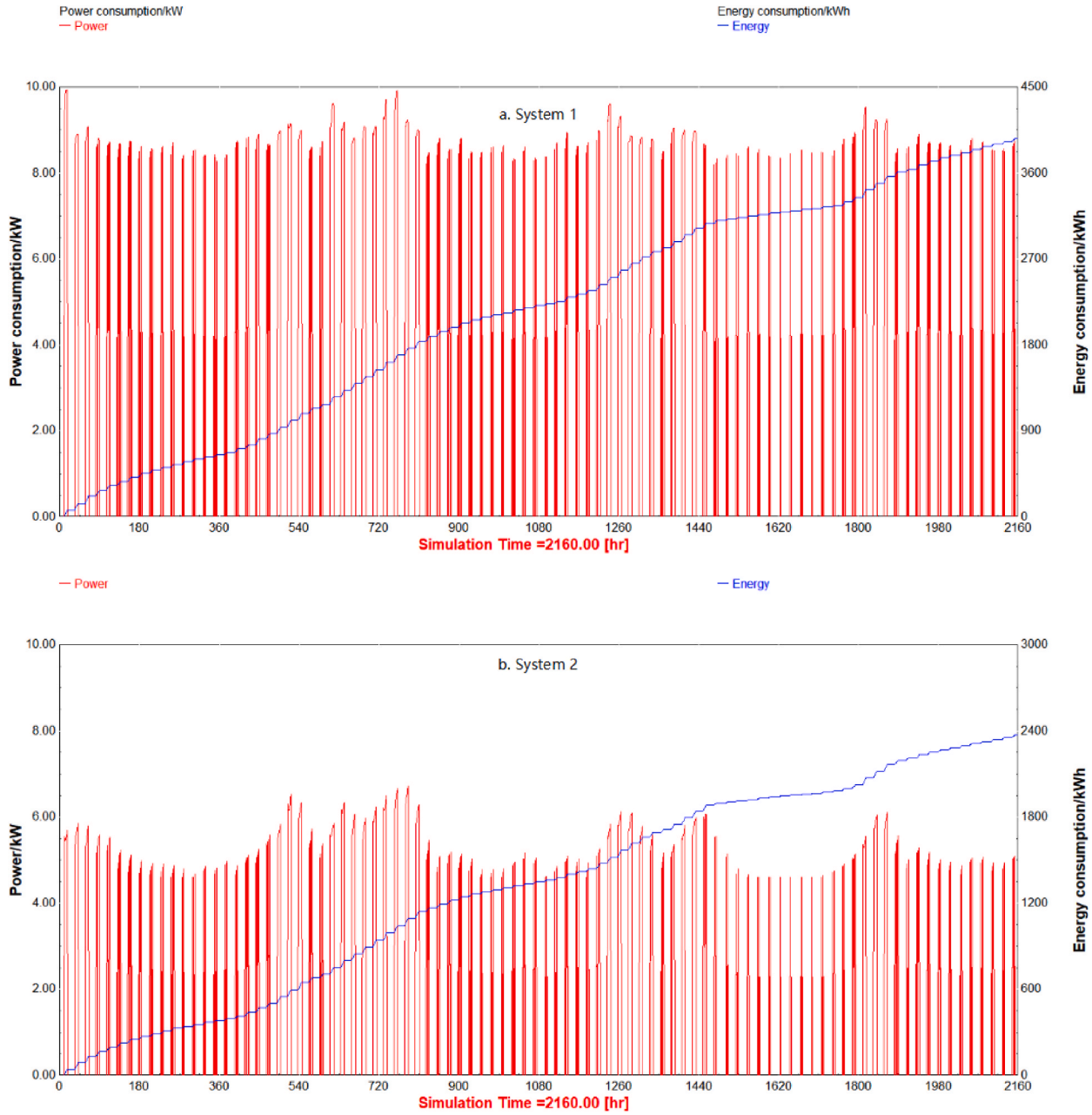

Fig. 7. Hourly power consumption and accumulated energy consumption of System 1 over 3 months.

In order to further investigate the performance of the RTDT-RAC system across different temperature ranges, additional sensitivity analyses will be conducted on the ESP for two specific room temperature ranges: the Refrigeration Range (2 °C–8 °C) and the Freezing Range (−24 °C to −18 °C). To adequately meet the cooling capacity requirements within each temperature range, it is necessary to adjust the rated total cooling capacities of Systems 1 and 2 to appropriate and sufficient values tailored for these respective ranges. The rated total cooling capacities for the Refrigeration Range and the Freezing Range have been adjusted to 75 kW and 150 kW, respectively.

The sensitivity of ESP on variable room temperature setpoints across different regions within the Refrigeration Range and the Freezing Range are shown in Figs. 10 and 11, respectively. The study of these two room temperature ranges proves that the ESP of the RTDT-RAC system does indeed increase with the room temperature setpoint for all studied regions. Specifically for the Freezing Range, the increases of ESP for all regions are found to be gradual.

Table 5
Results of the case study.

System 1. Air-cooled RAC system			
Month	Energy consumption (kWh)	System cooling (kWh)	Monthly COP
January	1621.88	4020.00	2.48
February	1333.32	3370.00	2.53
March	1005.34	2560.00	2.55
System 2. RTDT-RAC system			
Month	**Energy consumption (kWh)**	**System cooling (kWh)**	**Monthly COP**
January	986.31	4588.97	5.21
February	792.51	3763.65	5.42
March	598.65	2921.13	5.66
Comparison			
Month	**Energy-savings (kWh) by System 2**	**Energy Saving Percentage (ESP, %)**	
January	635.57	39.19	
February	540.81	40.56	
March	406.70	40.45	
Sum	1583.08	–	
Average	527.69	40.07	

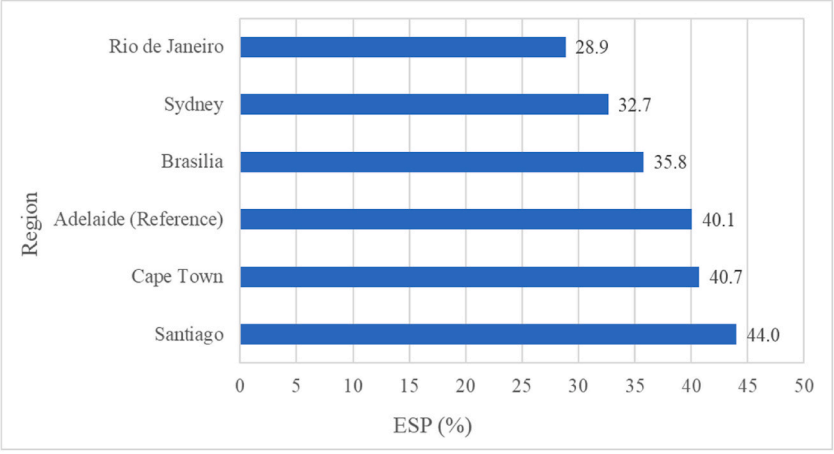

Fig. 8. Energy Saving Percentage (ESP) of the RTDT-RAC system across varied locations.

6.3. *RHP radiative surface area*

The impact of the RHP radiative surface (thermal collector component in TRNSYS) area on the ESP in different cities testing the RTDT-RAC system has been studied. In addition, the RTDT-RAC system is with a constant cooling capacity of 28.5 kW. As shown in Fig. 12, there are certain thresholds for the RHP radiative surface area that must be met in order to achieve positive ESPs across all the studied regions. If the RHP radiative surface area falls below these thresholds, the ESPs becomes negative. This is because when the RHP radiative surface is too small, the heat dissipation from the RTDT water to the ambient air may be insufficient, resulting in the RTDT water temperature being higher than the ambient temperature. Consequently, the performance and efficiency of the RTDT-RAC system may be lower than that of the reference system. To ensure positive ESPs in all regions, it is recommended that the minimum RHP radiative surface area should be approximately 2.2 m^2. For normalization, the minimum ratio of RHP radiative surface area to cooling capacity is around 0.077 m^2/kW.

Fig. 12 also reveals that when the RHP radiative surface area increases, the ESP experiences a rapid increase initially, provided that the area is within the range of 0 m^2–5 m^2. With a larger surface area, the system can more effectively dissipate heat from the RTDT to surroundings through the RHP, resulting in a lower water temperature and an improved energy efficiency of the RTDT-RAC system. This is particularly evident in the early stages when the surface area is relatively small, as even a modest increase in area can lead to a significant improvement in the system efficiency.

However, if the RHP radiative surface area continues to increase beyond 5 m^2, the increase rate in ESP becomes less pronounced. This diminishing return effect suggests that beyond 5 m^2, further increases in the surface area may provide only marginal benefits in the ESP. Moreover, when the RHP radiative surface area exceeds 20 m^2, the increase rate decreases further, leading to a flattening of the curve. It is found that the ESP can only increase by 0.1 for each 1 m^2 increase in the RHP radiative surface area when above 20 m^2.

These findings indicate the importance of carefully considering the size of the RHP radiative surface in relation to energy-savings.

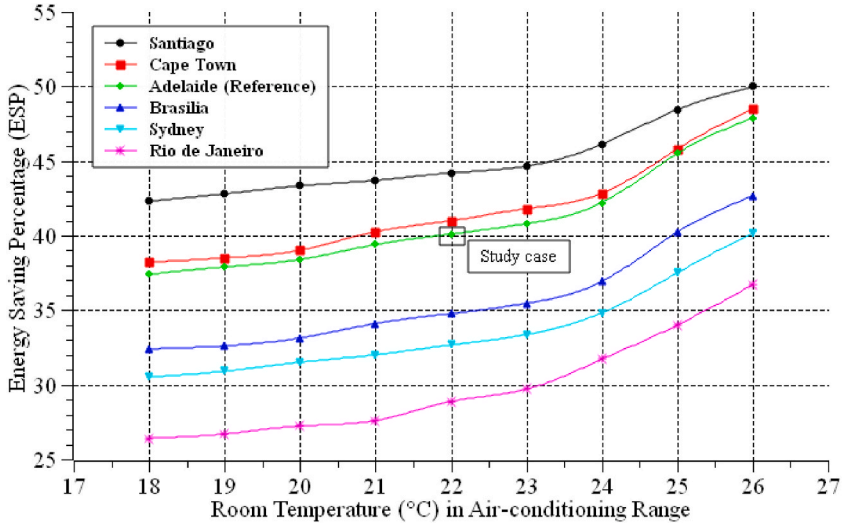

Fig. 9. Energy Saving Percentage (ESP) of the RTDT-RAC system across different regions at variable room temperature setpoints within the Air-conditioning Range 18 °C–26 °C.

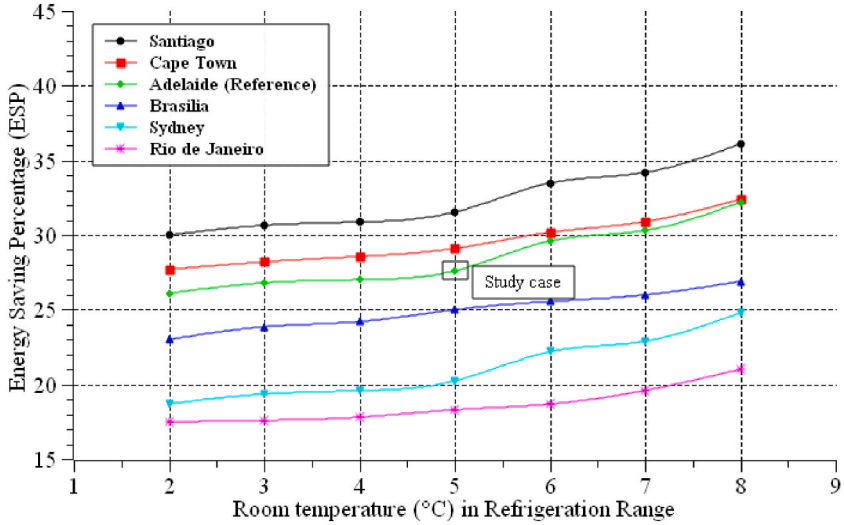

Fig. 10. Energy Saving Percentage (ESP) of the RTDT-RAC system across different regions at variable room temperature setpoints within the Refrigeration Range from 2 °C to 8 °C.

An undersized RHP radiative surface may cause negative ESP of the RTDT-RAC system. In contrast, oversizing the surface area may result in unnecessary costs without proportional gains in ESP. To balance both a high ESP and a high ESP increase rate, a radiative surface area of 5 m^2 can be considered as a potential optimal point.

7. Conclusions

In this paper, a case study was conducted using TRNSYS to compare the proposed RTDT-RAC system with a reference Air-cooled RAC system under summer weather conditions in Adelaide, Australia. In addition to the case study, a parametric analysis was conducted to investigate the impacts of various parameters on the RTDT-RAC system's performance. The following conclusions can be drawn.

- The RTDT-RAC system exhibited an improvement in achieving a lower room temperature than the reference system.
- On average, the RTDT-RAC system demonstrated a higher hourly COP at 5.34 than the reference system.
- The RTDT-RAC system provided more cooling energy for conditioning the room while consuming up to 40 % energy less than the reference system.

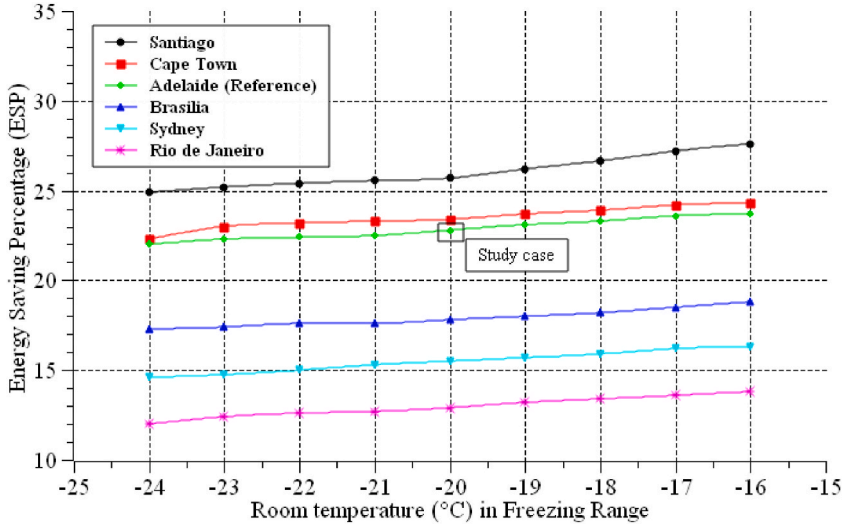

Fig. 11. Energy Saving Percentage (ESP) of the RTDT-RAC system across different regions at variable room temperature setpoints within the Freezing Range from −24 °C to −18 °C.

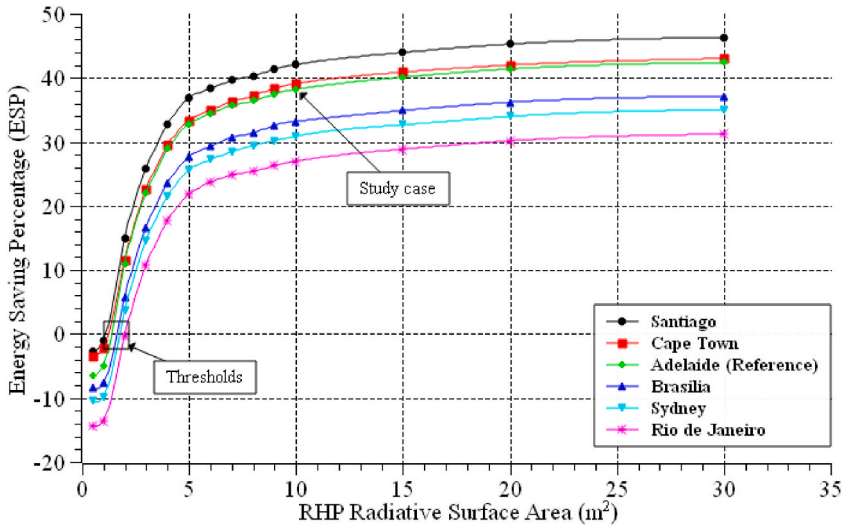

Fig. 12. Energy Saving Percentage (ESP) of the RTDT-RAC system across different regions with varied RHP radiative surface areas.

- The RTDT-RAC system at a location with a larger day and night ambient temperature difference is deemed to have a higher Energy Saving Percentage (ESP). Among the studied cities, Santiago showed the highest ESP at 44 %.
- Increasing the room temperature setpoint resulted in an increase in the ESP of the RTDT-RAC system, which indicates its potential to outperform the reference system in energy-savings.
- Thresholds for the RHP radiative surface area were found to achieve positive ESPs across all studied regions. Given with a 50 m^3 RTDT and a constant cooling capacity of 28.5 kW, it is recommended that the RHP radiative surface area should be at least 2.2 m^2 to ensure positive ESPs in all regions.
- Increasing the RHP radiative surface area could also lead to an increase in the ESP, but beyond 5 m^2, the increase rate diminishes and trends to zero. For a 50 m^3 RTDT, the optimal RHP radiative surface area is considered to be 5 m^2.

These findings highlight the potential of the RTDT-RAC system to achieve energy-savings, particularly in regions with larger day and night ambient temperature differences. The results also emphasise the importance of optimising parameters such as the room temperature setpoint and radiative surface area to maximise the energy efficiency of the RTDT-RAC system.

On the other hand, this study, based on TRNSYS simulation, involves numerous assumptions and simplifications, while it requires experimental validation to ensure that the simulation can accurately represent the RTDT-RAC system performance. The study has not considered the economic feasibility of implementing the RTDT-RAC system on a larger scale. Thus, scale-up studies and cost-benefit

analysis can be addressed in future research.

Author statement

We declare that this manuscript is original, has not been published before and is not currently being considered for publication elsewhere.

We also confirm that the manuscript has been read and approved by all named authors and that there are no other persons who satisfied the criteria for authorship but are not listed. We further confirm that the order of authors listed in the manuscript has been approved by all of us.

We understand that Mingzhen Wang is the sole contact for the Editorial process. He is responsible for communicating with the other authors about progress, submissions of revisions and final approval of proofs.

Declaration of competing interest

The authors declare the following financial interests/personal relationships which may be considered as potential competing interests: Eric Jing Hu has patent A HEAT TRANSFER ARRANGEMENT FOR IMPROVED ENERGY EFFICIENCY OF AN AIR CONDITIONING SYSTEM–A thermal 'Diode Tank' issued to AU 2014202998 Al.

Data availability

Data will be made available on request.

Acknowledgement

The authors sincerely thank the University of Adelaide for providing a University of Adelaide Research Scholarship for conducting this study.

Nomenclature

A	Area (m^2)
Q	Cooling energy (kJ)
$\dot{Q}$	Cooling power (kW)
T	Temperature (°C or K)
t	time (hr or sec)
W	Energy (kJ)
$\dot{W}$	Power (kW)

Subscripts

a	Air-cooled system (System 1)
blower	Blower
c1	Compressor of System 1
c2	Compressor of System 2
cooling1	Provided cooling of System 1
cooling2	Provided cooling of System 2
fan_in	Indoor fan
fan_out	Outdoor fan
saved	Savings
system1	System 1
system2	System 2
w	Water-cooled system (System 2)
waterpump	Water pump

Abbreviations

CCHP	Combined Cooling and Heating Power
COP	Coefficient of Performance
GSHP	Ground-sourced heat pump
PCM	Phase Change Materials
RAC	Refrigeration and Air-conditioning
RHP	Radiation-enhanced/Radiative Heat pipe
RTDT	Radiation-enhanced Thermal Diode Tank
TDT	Thermal Diode Tank

TDT-RAC Thermal Diode Tank assisted Refrigeration and Air-conditioning
TRNSYS Transient System Simulation Program

References

[1] S.F. Li, Z. hua Liu, X.J. Wang, A comprehensive review on positive cold energy storage technologies and applications in air conditioning with phase change materials, Appl. Energy 255 (Dec. 2019), 113667, https://doi.org/10.1016/J.APENERGY.2019.113667.
[2] A. Kumbhar, N. Gulhane, S. Pandure, Effect of various parameters on working condition of chiller, Energy Proc. 109 (Mar. 2017) 479–486, https://doi.org/10.1016/J.EGYPRO.2017.03.076.
[3] K.A. Jahangeer, A.A.O. Tay, M. Raisul Islam, Numerical investigation of transfer coefficients of an evaporatively-cooled condenser, Appl. Therm. Eng. 31 (10) (Jul. 2011) 1655–1663, https://doi.org/10.1016/J.APPLTHERMALENG.2011.02.007.
[4] E. Hajidavalloo, H. Eghtedari, Performance improvement of air-cooled refrigeration system by using evaporatively cooled air condenser, Int. J. Refrig. 33 (5) (Aug. 2010) 982–988, https://doi.org/10.1016/J.IJREFRIG.2010.02.001.
[5] P. Sarntichartsak, S. Thepa, Modeling and experimental study on the performance of an inverter air conditioner using R-410A with evaporatively cooled condenser, Appl. Therm. Eng. 51 (1–2) (Mar. 2013) 597–610, https://doi.org/10.1016/J.APPLTHERMALENG.2012.08.063.
[6] T. Wang, C. Sheng, A.G.A. Nnanna, Experimental investigation of air conditioning system using evaporative cooling condenser, Energy Build. 81 (Oct. 2014) 435–443, https://doi.org/10.1016/J.ENBUILD.2014.06.047.
[7] E. Hajidavalloo, Application of evaporative cooling on the condenser of window-air-conditioner, Appl. Therm. Eng. 27 (11–12) (Aug. 2007) 1937–1943, https://doi.org/10.1016/J.APPLTHERMALENG.2006.12.014.
[8] F.W. Yu, K.T. Chan, Application of direct evaporative coolers for improving the energy efficiency of air-cooled chillers, J. Sol. Energy Eng. 127 (3) (Aug. 2005) 430–433, https://doi.org/10.1115/1.1866144.
[9] B.J. Kim, S.Y. Jo, J.W. Jeong, Energy performance enhancement in air-source heat pump with a direct evaporative cooler-applied condenser, Case Stud. Therm. Eng. 35 (Jul. 2022), 102137, https://doi.org/10.1016/J.CSITE.2022.102137.
[10] W. Ketwong, T. Deethayat, T. Kiatsiriroat, Performance enhancement of air conditioner in hot climate by condenser cooling with cool air generated by direct evaporative cooling, Case Stud. Therm. Eng. 26 (Aug. 2021), 101127, https://doi.org/10.1016/J.CSITE.2021.101127.
[11] P. Martínez, J. Ruiz, C.G. Cutillas, P.J. Martínez, A.S. Kaiser, M. Lucas, Experimental study on energy performance of a split air-conditioner by using variable thickness evaporative cooling pads coupled to the condenser, Appl. Therm. Eng. 105 (Jul. 2016) 1041–1050, https://doi.org/10.1016/J.APPLTHERMALENG.2016.01.067.
[12] M. Kharseh, M. Al-Khawaja, M.T. Suleiman, Potential of ground source heat pump systems in cooling-dominated environments: residential buildings, Geothermics 57 (Sep. 2015) 104–110, https://doi.org/10.1016/J.GEOTHERMICS.2015.06.009.
[13] J. Luo, J. Rohn, M. Bayer, A. Priess, L. Wilkmann, W. Xiang, Heating and cooling performance analysis of a ground source heat pump system in Southern Germany, Geothermics 53 (Jan. 2015) 57–66, https://doi.org/10.1016/J.GEOTHERMICS.2014.04.004.
[14] P. Christodoulides, L. Aresti, G. Florides, Air-conditioning of a typical house in moderate climates with ground source heat pumps and cost comparison with air source heat pumps, Appl. Therm. Eng. 158 (Jul. 2019), 113772, https://doi.org/10.1016/J.APPLTHERMALENG.2019.113772.
[15] Z. Qiao, et al., Performance assessment of ground-source heat pumps (GSHPs) in the Southwestern and Northwestern China: in situ measurement, Renew. Energy 153 (Jun. 2020) 214–227, https://doi.org/10.1016/J.RENENE.2020.02.024.
[16] A. Girard, E.J. Gago, T. Muneer, G. Caceres, Higher ground source heat pump COP in a residential building through the use of solar thermal collectors, Renew. Energy 80 (Aug. 2015) 26–39, https://doi.org/10.1016/J.RENENE.2015.01.063.
[17] P. Christodoulides, L. Aresti, G. Florides, Air-conditioning of a typical house in moderate climates with ground source heat pumps and cost comparison with air source heat pumps, Appl. Therm. Eng. 158 (Jul. 2019), 113772, https://doi.org/10.1016/J.APPLTHERMALENG.2019.113772.
[18] P. Saji Raveendran, S. Joseph Sekhar, Experimental studies on the performance improvement of household refrigerator connected to domestic water system with a water-cooled condenser in tropical regions, Appl. Therm. Eng. 179 (Oct. 2020), 115684, https://doi.org/10.1016/j.applthermaleng.2020.115684.
[19] F. Wei, B. Wang, Z. Cheng, M. Cui, Experimental research on vapor-injected water source heat pump using R1234ze(E), Appl. Therm. Eng. 229 (Jul. 2023), 120595, https://doi.org/10.1016/J.APPLTHERMALENG.2023.120595.
[20] R. López-Zavala, et al., Novel desalination system that uses product water to generate cooling through a barometric ejector-condenser, Energy 276 (Aug. 2023), 127536, https://doi.org/10.1016/j.energy.2023.127536.
[21] M. Wang, E. Hu, L. Chen, Energy-saving potential of thermal diode tank assisted refrigeration and air-conditioning systems, Energies 15 (1) (Dec. 2021) 206, https://doi.org/10.3390/en15010206.
[22] M. Wang, E. Hu, L. Chen, Radiation-enhanced thermal diode tank (RTDT) for refrigeration and air-conditioning (RAC) systems, Int. J. Refrig. 146 (Feb. 2023) 237–247, https://doi.org/10.1016/J.IJREFRIG.2022.11.004.
[23] Y. Allouche, S. Varga, C. Bouden, A. Oliveira, A Trnsys simulation of a solar-driven ejector air conditioning system with an integrated PCM cold storage, AIP Conf. Proc. 1814 (1) (Feb. 2017), 020021, https://doi.org/10.1063/1.4976240.
[24] J.A. Aguilar-Jiménez, N. Velázquez, R. López-Zavala, L.A. González-Uribe, R. Beltrán, L. Hernández-Callejo, Simulation of a solar-assisted air-conditioning system applied to a remote school, Appl. Sci. 9 (16) (Aug. 2019) 3398, https://doi.org/10.3390/APP9163398, 2019, Vol. 9, Page 3398.
[25] R. Chargui, H. Sammouda, Modeling of a residential house coupled with a dual source heat pump using TRNSYS software, Energy Convers. Manag. 81 (May 2014) 384–399, https://doi.org/10.1016/J.ENCONMAN.2014.02.040.
[26] R. Chargui, H. Sammouda, A. Farhat, Geothermal heat pump in heating mode: modeling and simulation on TRNSYS, Int. J. Refrig. 35 (7) (Nov. 2012) 1824–1832, https://doi.org/10.1016/J.IJREFRIG.2012.06.002.
[27] S. Bordignon, G. Emmi, A. Zarrella, M. de Carli, Energy analysis of different configurations for a reversible ground source heat pump using a new flexible TRNSYS Type, Appl. Therm. Eng. 197 (Oct. 2021), 117413, https://doi.org/10.1016/J.APPLTHERMALENG.2021.117413.
[28] G. Hou, H. Taherian, L. Li, A predictive TRNSYS model for long-term operation of a hybrid ground source heat pump system with innovative horizontal buried pipe type, Renew. Energy 151 (May 2020) 1046–1054, https://doi.org/10.1016/J.RENENE.2019.11.113.
[29] S.N. Al-Saadi, Z. Zhai, A new validated TRNSYS module for simulating latent heat storage walls, Energy Build. 109 (Dec. 2015) 274–290, https://doi.org/10.1016/J.ENBUILD.2015.10.013.
[30] D. Brough, J. Ramos, B. Delpech, H. Jouhara, Development and validation of a TRNSYS type to simulate heat pipe heat exchangers in transient applications of waste heat recovery, International Journal of Thermofluids 9 (Feb. 2021), 100056, https://doi.org/10.1016/J.IJFT.2020.100056.
[31] M.S. Ahamed, H. Guo, K. Tanino, Modeling heating demands in a Chinese-style solar greenhouse using the transient building energy simulation model TRNSYS, J. Build. Eng. 29 (May 2020), 101114, https://doi.org/10.1016/J.JOBE.2019.101114.
[32] F. Kuznik, J. Virgone, K. Johannes, Development and validation of a new TRNSYS type for the simulation of external building walls containing PCM, Energy Build. 42 (7) (Jul. 2010) 1004–1009, https://doi.org/10.1016/J.ENBUILD.2010.01.012.
[33] H. Fang, W. Wang, J. Liu, L. Zhang, Operation analysis of a compound air conditioning system using measurement and simulation, Procedia Eng. 205 (Jan. 2017) 1454–1460, https://doi.org/10.1016/J.PROENG.2017.10.360.
[34] C.J. Banister, W.R. Wagar, M.R. Collins, Validation of a single tank, multi-mode solar-assisted heat pump TRNSYS model, Energy Proc. 48 (2014) 499–504, https://doi.org/10.1016/J.EGYPRO.2014.02.059.

[35] X. Lin, Y. Pan, Z. Huang, Emulation of HVAC control systems based on TRNSYS, Journal of Building Energy Efficiency 38 (228) (2010), https://doi.org/10.3969/j.issn.1673-7237.2010.02.015.
[36] P. Haurant, C. Ménézo, L. Gaillard, P. Dupeyrat, A numerical model of a solar domestic hot water system integrating hybrid photovoltaic/thermal collectors, Energy Proc. 78 (Nov. 2015) 1991–1997, https://doi.org/10.1016/J.EGYPRO.2015.11.391.
[37] J. Bony, S. Citherlet, Numerical model and experimental validation of heat storage with phase change materials, Energy Build. 39 (10) (Oct. 2007) 1065–1072, https://doi.org/10.1016/J.ENBUILD.2006.10.017.
[38] D.N. Nkwetta, P.E. Vouillamoz, F. Haghighat, M. El-Mankibi, A. Moreau, A. Daoud, Impact of phase change materials types and positioning on hot water tank thermal performance: using measured water demand profile, Appl. Therm. Eng. 67 (1–2) (Jun. 2014) 460–468, https://doi.org/10.1016/J.APPLTHERMALENG.2014.03.051.
[39] TRNSYS - Official Website. https://sel.me.wisc.edu/trnsys/.
[40] M. Wang, E. Hu, L. Chen, Performance Simulation Model of a Radiation-Enhanced Thermal Diode Tank-Assisted Refrigeration and Air-Conditioning (RTDT-RAC) System: A Novel Cooling System, Energies 16 (Sept, 2023) 6506. https://doi.org/10.3390/en16186506.